

Au wetting and nanoparticle stability on GaAs(111)B

E. Hilner, A. Mikkelsen,^{a)} J. Eriksson, J. N. Andersen, and E. Lundgren
Department of Synchrotron Radiation Research, Institute of Physics, University of Lund, S-221 00 Lund, Sweden

A. Zakharov
MAX-lab, University of Lund, S-221 00 Lund, Sweden

H. Yi and P. Kratzer
Fritz-Haber-Institut der MPG, Faradayweg 4-6, D-14195 Berlin, Germany

(Received 28 June 2006; accepted 14 November 2006; published online 21 December 2006)

Au nanoparticles and Au films for growth of nanowires on the GaAs(111)B surface have been studied by a combination of experimental and theoretical techniques. If Au is present in either form, annealing to temperatures relevant for nanowire growth results in the formation of a thin Au wetting layer. Based on density functional theory calculations and experimental data, a structural model is proposed with an Au atom on every third threefold hollow hcp site of the Ga lattice. The authors observe that the stability of Au nanoparticles is governed by the presence of the wetting layer and outdiffusion of Au from the nanoparticles. © 2006 American Institute of Physics.

[DOI: 10.1063/1.2416315]

The potential of freestanding semiconductor nanowires as tools and devices in physics, chemistry, and biology is enormous.¹⁻⁴ The nanowires are attractive as their shape, size, and composition can be varied in a reproducible manner and complex heterostructures can be formed inside the wires.² However, it has recently been shown experimentally that the conventional picture of semiconductor nanowire growth has significant shortcomings for both Si and III-V nanowires.⁵⁻⁸ This is perhaps not surprising as the original models are based on experimental data from the 60s,⁹ where many of the modern experimental and theoretical tools were not available. Hence it is of great importance to reexamine nanowire nucleation with the atomic-scale tools developed more recently.

Semiconductor nanowire growth is very often catalyzed by Au nanoparticles, which act to promote one-dimensional growth at the semiconductor/particle interface. Consequently Au nanoparticles play a crucial role in controlling the growth of the wires. Their position determines the position (and hence the density) of the nanowires, and their diameters determines the diameter of the nanowires. Further, as substrate diffusion strongly influences the growth, any alterations of the surface structure due to the presence of Au can dramatically change diffusion coefficients, leading to unexpected growth behavior. Interestingly most models of nanowire growth implicitly assume that no Au diffusion in and out of the particle occurs and that the substrate is free of Au.⁹⁻¹² In this letter we show that these assumptions are incorrect for GaAs(111). Au can migrate even from preadsorbed Au particles and will form a thin wetting layer on the GaAs. In this context we note that little is known about the interaction of Au with GaAs surfaces; so far it has been studied on the atomic scale only for GaAs(110) and (100).^{13,14}

Several methods are used for forming the Au nanoparticle seed: In the simplest case, Au is deposited as a homogeneous film, which upon annealing condenses to Au droplets.^{10,11,15} Size-selected Au seed particles can also be prepared directly, for example, by aerosol methods¹⁶ or

lithography,¹⁷ thereby achieving lateral and size ordering. In the present letter we will explore both annealing of Au films and direct aerosol deposition of Au nanoparticles.

Because GaAs nanowires grow most readily in the $\langle 111 \rangle B$ directions, the GaAs(111)B substrate has been used for the vast majority of GaAs nanowire growth studies.² Thus we focus on how Au adsorption on the GaAs(111)B surface affects the surface structure, and hence diffusion and nanowire growth.

In this letter, we report scanning tunneling microscopy (STM) and low energy electron diffraction/microscopy (LEED/LEEM) measurements of the GaAs(111)B surface morphology and structure after depositing Au either homogeneously or as aerosol nanoparticles, followed by annealing to temperatures of 450–700 °C relevant for nanowire growth.^{2,10,11,15} Both Au films and Au nanoparticles affect the surface in a similar way after the annealing, inducing a $(\sqrt{3} \times \sqrt{3})R30^\circ$ structure. High resolution STM images and density functional theory (DFT) calculations are used to establish a model for the structure of this Au wetting layer on the GaAs(111)B surface. We further observe that the Au particle density will only become stable after the formation of the wetting layer, and that Au diffusion on the substrate is faster than detachment from the Au particle.

All measurements were performed in ultrahigh vacuum with commercial Omicron LEED and STM under a base pressure below 1×10^{-10} mbar. All STM images were obtained in constant current mode. LEEM measurements were carried out using a commercial Elmitec SPLEEM system at MAX-lab. The samples used in this study were all cut from the same crystal wafer, *n*-doped GaAs(111)B. Au films were deposited in vacuum using a home-built evaporator, calibrated by monitoring island growth during the formation of the first Au layer on GaAs at room temperature. Alternatively, size-selected Au aerosol nanoparticles with a diameter of nominally 50 nm were deposited directly *ex situ* on the GaAs(111)B substrate as described elsewhere.¹⁶ Calculations of the geometric and electronic structures of both the clean and the Au-covered GaAs(111)B surfaces were performed in

^{a)}Electronic mail: anders.mikkelsen@sljus.lu.se

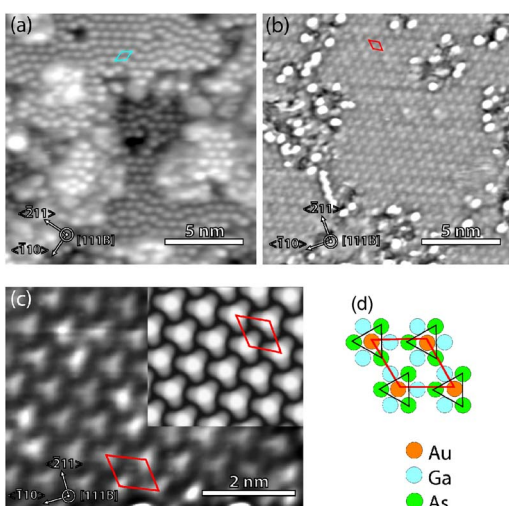


FIG. 1. (Color online) (a) STM image ($16 \times 16 \text{ nm}^2$) of the clean GaAs(111)*B* surface ($U=1.4 \text{ V}$). Gray scale extends over 10 \AA and (b) STM image ($16 \times 16 \text{ nm}^2$) of the clean GaAs(111)*B* surface with 2.5 ML Au film annealed to $600 \text{ }^\circ\text{C}$ ($U=-0.6 \text{ V}$). Gray scale extends over 4 \AA . The Au-induced $(\sqrt{3} \times \sqrt{3})R30^\circ$ cell is indicated. (c) STM image ($7 \times 5 \text{ nm}^2$) of triangular structural units on the surface ($U=-0.6 \text{ V}$). Gray scale extend over 1 \AA . The inset shows the simulated STM images from DFT calculations. (d) Model of Au atoms occupying every third threefold hollow site giving rise to these small triangles

the framework of density functional theory within the generalized-gradient approximation.¹⁸ The electronic structure was calculated with the program CASTEP,¹⁹ using a plane-wave expansions of the wave functions with a cutoff energy of 320 eV in combination with ultrasoft pseudopotentials. The GaAs(111)*B* surface was modeled using periodic slabs of six GaAs bilayers, separated by a vacuum region of 13 \AA . We fix the bottom two bilayers and the H atoms used to terminate the slab, and relax the remaining atoms until all the forces were smaller than 0.01 eV/\AA . After structural relaxation, contour plots of a suitably defined local density of states were extracted, corresponding to filled-state STM images in constant-current mode.²⁰

After annealing the clean GaAs(111)*B* sample to $550 \text{ }^\circ\text{C}$ a sharp (1×1) LEED pattern could be observed. Since this surface reconstruction did not change further after annealing to temperatures up to $600 \text{ }^\circ\text{C}$, we conclude that the observed structure is the so-called $(1 \times 1)_{\text{HT}}$ reconstruction.²¹ The STM measurements revealed a surface morphology with many small, but flat patches. The STM image in Fig. 1(a) shows that the patches consist of protrusions which have only very local ordering of up to a few (2×2) unit cells.

In separate experiments, 0.5 and 2.5 ML (monolayer) of Au were deposited at room temperature on the clean surface. After the samples had been annealed to $600 \text{ }^\circ\text{C}$ for 1 min a $(\sqrt{3} \times \sqrt{3})R30^\circ$ LEED pattern could be observed for both Au coverages. In the STM images on Fig. 1(b) it is observed that the overall morphology of the surface changed as compared to the clean surface. The surface now consists of much larger terraces with an ordered $(\sqrt{3} \times \sqrt{3})R30^\circ$ structure, with disordered patches in between.

From high-resolution STM images as seen in Fig. 1(c), we find that the structural units of the $(\sqrt{3} \times \sqrt{3})R30^\circ$ are triangular with bright centers. The areal density of the triangular units, together with our observation that the reconstruction appears already for 0.5 ML of Au deposited, strongly suggests that each unit contains one Au atom. On the basis of

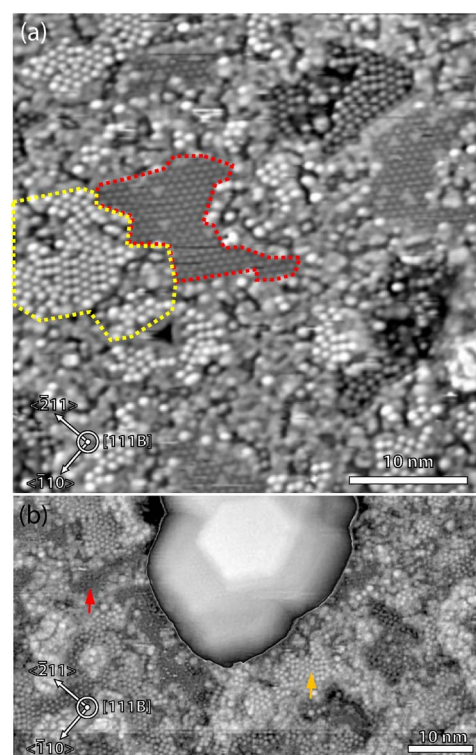


FIG. 2. (Color online) (a) STM image ($40 \times 40 \text{ nm}^2$) of the GaAs(111)*B* surface with $0.5 \text{ Au particles}/\mu\text{m}^2$ after annealing to $600 \text{ }^\circ\text{C}$. The yellow/red regions are regions of clean GaAs(111)*B* and the $(\sqrt{3} \times \sqrt{3})R30^\circ$ -Au structure, respectively ($U=2.0 \text{ V}$). Gray scale extends over 9 \AA . (b) STM image ($73 \times 42 \text{ nm}^2$) of the GaAs(111)*B* surface with a Au particle after annealing to $600 \text{ }^\circ\text{C}$ ($U=2.4 \text{ V}$). Regions of clean GaAs(111)*B* and the $(\sqrt{3} \times \sqrt{3})R30^\circ$ -Au structure can be seen near the particle as indicated by the yellow and red arrows, respectively. As the height of the Au particle is 30 \AA , the gray scale of the particle has been compressed to also allow the structure on the substrate to be seen.

our results from the STM and LEED measurements we suggest a model for the adsorption sites of the Au atoms on the surface [Fig. 1(d)]. In this model the Au atoms preferably adsorb on every third hcp threefold hollow site of the Ga lattice.

The simulated STM images for the proposed structural model [see inset in Fig. 1(c)] show excellent agreement with the measured images. The adsorption energy per Au atom on the ideally As-terminated, relaxed GaAs(111)*B* surface is 2.96 eV for this structure, slightly smaller than the (calculated) cohesive energy of bulk gold, $E_{\text{coh}}^{\text{Au}}=3.01 \text{ eV}$. However, such a wetting layer may still be thermodynamically stable in equilibrium with Au nanoparticles, since entropic contributions to the free energy favor spreading out of the gold onto the substrate. By simulating STM images of the clean GaAs(111)*B* surface, we also verified that the presence of Au is essential for obtaining the correct image: various assumed structures of the clean surface (Ga adatoms, As vacancies, As vacancies in combination with Ga trimers) yield STM images markedly different from the experimentally observed ones.

In the case of homogeneous Au deposition, the Au wetting layer remains after the film has condensed into Au droplets. Thus the interesting question arises whether a Au wetting layer will also form for preadsorbed Au particles (or Au patches) and if Au particles are stable without the presence of the Au structure. To investigate these issues, GaAs(111)*B* samples with preadsorbed 50 nm Au aerosol nanoparticles

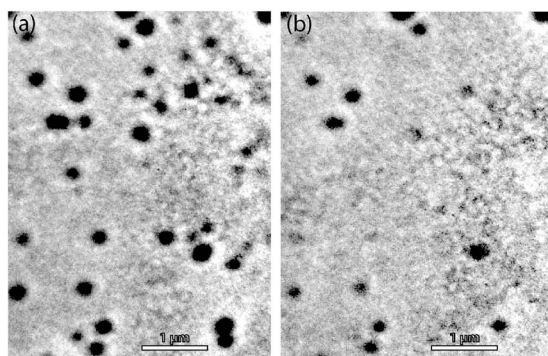


FIG. 3. $4 \times 5 \mu\text{m}^2$ LEEM images at 0.54 eV (mirror mode) of the same area of a GaAs(111)*B* surface with Au aerosol nanoparticles. (a) Immediately after reaching 700 °C. (b) After annealing at 700 °C for 300 s. The two images are drift corrected to show the same area of the surface.

(density of 5 particles/ μm^2) were annealed in a similar fashion as the samples with Au films. Again a $(\sqrt{3} \times \sqrt{3})R30^\circ$ phase was observed, which was found to be identical both structurally and morphologically to the structure on samples with annealed Au films. This shows that wetting of the whole surface will also occur upon annealing of local Au structures. Decreasing the particle density to 0.5 particles/ μm^2 and annealing the sample leads to an interesting change. Imaging the surface by STM, as seen in Fig. 2(a), we find a coexistence of the reconstruction of the clean GaAs(111)*B* surface with patches of the Au-induced $(\sqrt{3} \times \sqrt{3})R30^\circ$ reconstruction and disordered patches with a few protrusions in an arrangement similar as that of the protrusions on the clean surface.

Disordered patches similar to the ones found in between the $(\sqrt{3} \times \sqrt{3})R30^\circ$ structure are also observed on the clean surface with no Au present. The coverage and appearance of the disordered patches show no special dependence on the amount of Au adsorbed and no changes are observed by adsorption of more than 0.5 ML Au. Therefore we conclude that only small amounts of Au can be present in the disordered regions.

Probing regions close to an Au particle as seen in Fig. 2(b) we find no notable difference in the density of reconstructed regions close to and far away from the Au particles. This finding implies a large mobility of Au atoms on the surface compared to the rate of Au detachment from the nanoparticle. The high surface mobility of Au is in agreement with the DFT calculations, which determine the diffusion barrier for Au on GaAs(111)*B* to be only 0.2 eV.

Finally we have studied the stability of the Au nanoparticles upon annealing. This was done by heating the GaAs(111)*B* surface with Au aerosol nanoparticles up to 700 °C and keeping it at this temperature while simultaneously recording LEEM images as seen in Fig. 3. From these images it can be seen that about 60% of the particles disappear. The total amount of Au left in the form of particles becomes smaller after annealing, consistent with the spreading of some of the Au from the particles onto the surface as a thin wetting layer. Indeed, after prolonged annealing the Au particles stop to shrink or disappear as found by a second annealing series to 700 °C of the same sample. On samples where the total amount of Au present as particles could only cover up to 80% of the surface with the $(\sqrt{3} \times \sqrt{3})R30^\circ$ struc-

ture, very few particles were observed after prolonged annealing. Thus one can view the 1/3 ML Au layer as a very thin wetting layer, necessary for the thermodynamic stability of the Au particles on the surface. Finally it can be noted that at nanowire growth temperatures (below 700 °C) the disappearance of Au particles and Au outdiffusion will be significantly slower; however, for prolonged growth times it can explain needle formation where the catalyzing particle is seen to slowly disappear.¹⁵

We have studied the GaAs(111)*B* surface with Au deposited either homogeneously or as nanoparticles, and found the presence of Au in either form to give rise to a $(\sqrt{3} \times \sqrt{3})R30^\circ$ Au-induced surface reconstruction. In the structural model supported by our DFT calculations for an Au coverage of 1/3 ML, Au atoms are adsorbed at every third threefold hollow hcp site of the Ga lattice. We find that Au particle stability depends on the presence of this wetting layer.

The work at Lund University was performed within the Nanometer Structure Consortium, and was supported by the Swedish Research Council (VR), the Swedish Foundation for Strategic Research (SSF), the Crafoord Foundation, and the Knut and Alice Wallenberg Foundation. The authors acknowledge help from the MAX-lab staff and financial support by the SANDiE network.

¹G. Zheng, F. Patolsky, Y. Cui, W. U. Wang, and C. M. Lieber, *Nat. Biotechnol.* **23**, 1294 (2005); Y. Cui, Q. Wei, H. Park, and C. M. Lieber, *Mater. Today* **23**, 20 (2005), and references therein.

²L. Samuelson, *Mater. Today* **6**(10), 22 (2003), and references therein.

³H. Pettersson, J. Trädgårdh, A. I. Persson, L. Landin, D. Hessman, and L. Samuelson, *Nano Lett.* **6**, 229 (2006).

⁴Y. Huang, X. Duan, Y. Cui, L. J. Lauhon, K.-H. Kim, and C. M. Lieber, *Science* **294**, 1313 (2001).

⁵J. B. Hannon, S. Kodambaka, F. M. Ross, and R. M. Tromp, *Nature (London)* **440**, 69 (2006).

⁶S. Kodambaka, J. Tersoff, M. C. Reuter, and F. M. Ross, *Phys. Rev. Lett.* **96**, 096105 (2006).

⁷A. I. Persson, M. W. Larsson, S. Stenström, B. J. Ohlsson, L. Samuelson, and L. R. Wallenberg, *Nat. Mater.* **3**, 677 (2004).

⁸K. A. Dick, K. Deppert, T. Mårtensson, B. Mandl, L. Samuelson, and W. Seifert, *Nano Lett.* **5**, 761 (2005).

⁹R. S. Wagner, in *Whisker Technology*, edited by A. P. Levitt (Wiley, New York, 1970), p. 47.

¹⁰G. E. Cirlin, V. G. Dubrovskii, N. V. Sibirev, I. P. Soshnikov, Y. B. Samsonenko, A. A. Tonkikh, and V. M. Ustinov, *Semiconductors* **39**, 557 (2005).

¹¹V. G. Dubrovskii, G. E. Cirlin, I. P. Soshnikov, A. A. Tonkikh, N. V. Sibirev, Y. B. Samsonenko, and V. M. Ustinov, *Phys. Rev. B* **71**, 205325 (2005).

¹²L. E. Jensen, K. Deppert, T. Mårtensson, B. Mandl, L. Samuelson, and W. Seifert, *Nano Lett.* **4**, 1961 (2004).

¹³R. M. Feenstra, *J. Vac. Sci. Technol. B* **7**, 925 (1989).

¹⁴A. A. Bonapasta, G. Scavia, and F. Buda, *Surf. Sci.* **520**, 53 (2002).

¹⁵K. Haraguchi, T. Katsuyama, K. Hiruma, and K. Ogawa, *Appl. Phys. Lett.* **60**, 745 (1992).

¹⁶M. H. Magnusson, K. Deppert, J.-O. Malm, J.-O. Bovin, and L. Samuelson, *J. Nanopart. Res.* **1**, 243 (1999).

¹⁷T. Mårtensson, P. Carlberg, M. Borgström, L. Montelius, W. Seifert, and L. Samuelson, *Nano Lett.* **4**, 699 (2004).

¹⁸J. P. Perdew, K. Burke, and M. Ernzerhof, *Phys. Rev. Lett.* **77**, 3865 (1996).

¹⁹M. D. Segall, P. J. D. Lindan, M. J. Probert, C. J. Pickard, P. J. Hasnip, S. J. Clark, and M. C. Payne, *J. Phys.: Condens. Matter* **14**, 2717 (2002).

²⁰J. Tersoff and D. R. Hamann, *Phys. Rev. B* **31**, 805 (1985).

²¹J. M. C. Thornton, D. A. Woolf, and P. Weightman, *Appl. Surf. Sci.* **123/124**, 115 (1998).